



HAL
open science

On the collapsing sandpile problem

Serge Dumont, Nouredine Igbida

► **To cite this version:**

Serge Dumont, Nouredine Igbida. On the collapsing sandpile problem. Communications on Pure and Applied Mathematics, 2011, 10 (2), pp.625-638. 10.3934/cpaa.2011.10.625 . hal-00936231

HAL Id: hal-00936231

<https://hal.science/hal-00936231>

Submitted on 16 Jul 2018

HAL is a multi-disciplinary open access archive for the deposit and dissemination of scientific research documents, whether they are published or not. The documents may come from teaching and research institutions in France or abroad, or from public or private research centers.

L'archive ouverte pluridisciplinaire **HAL**, est destinée au dépôt et à la diffusion de documents scientifiques de niveau recherche, publiés ou non, émanant des établissements d'enseignement et de recherche français ou étrangers, des laboratoires publics ou privés.

On the Collapsing Sandpile Problem

Serge DUMONT, Nouredine IGBIDA*

March 2008

Abstract

In this note, we are interested in the numerical analysis of the collapse of an unstable sandpile. By using the collapsing model introduced by Evans, Feldman and Garipey in [6], we give a description of the phenomena in terms of a composition of projections onto interlocked convex sets around the set of stable sandpiles.

1. Introduction and main results

We are interested in the collapse of an unstable sandpile; i.e. taking some sandpile with an unstable initial configuration, what is the final resting state of the sandpile after various avalanches. To describe the problem we need to use some function $u : \mathbb{R}^D \rightarrow \mathbb{R}$, the height function of the sandpile, where $D \geq 1$ (in practice $D = 2$). The stability constraint of the sandpile reads

$$(1) \quad |\nabla u| \leq 1,$$

and has the physical meaning that the sand cannot remain in equilibrium if the slope anywhere exceeds angle $\pi/4$. Now, if g represents the height of a starting unstable profile (assume for instance g is the profile of a wet sandpile) i.e.

$$L := \|\nabla g\|_\infty > 1,$$

then constraint (1) forces the height function to rearrange itself to achieve the profile in a stable configuration. Our main interest lies in the description of mapping $\mathbb{Q} : g \rightarrow \mathbb{Q}(g)$, where $\mathbb{Q}(g)$ is the final stable profile of the sandpile associated with the initial unstable one g .

*LAMFA, UPJV CNRS UMR 6140, Université de Picardie Jules Verne, 33 rue Saint Leu, 80038 Amiens, France. Email : [serge.dumont,nouredine.igbida]@u-picardie.fr

By using the Monge Kantorovich mass transfer theory, Evans, Feldman and Gariépy [6] introduced a simplistic model for the collapse of an unstable sandpile. It is given by the limit of the flow governed by the p -Laplacian, as $p \rightarrow \infty$:

$$(2) \quad \begin{cases} -u_t = \Delta_p u & \text{in } Q := (0, \infty) \times \Omega \\ u(0) = g & \text{in } \Omega. \end{cases}$$

Letting $p \rightarrow \infty$, one expects that the limit of solution u_p satisfies evolution equation (multivalued)

$$(3) \quad u_t \in \partial \mathbb{I}_K(u) \quad \text{in } Q,$$

where \mathbb{I}_K is defined by

$$\mathbb{I}_K(u) = \begin{cases} 0 & \text{if } u \in K \\ +\infty & \text{otherwise,} \end{cases}$$

$$K = \left\{ u \in W^{1,\infty}(\Omega) ; |\nabla u| \leq 1 \text{ a.e. } \Omega \right\}.$$

and the subdifferential operator $\partial \mathbb{I}_K$ is defined in $L^2(\Omega)$, by

$$h \in \partial \mathbb{I}_K(u) \Leftrightarrow h \in L^2(\Omega), u \in K \text{ and } \int_{\Omega} h(z - u) \leq 0 \quad \forall z \in L^2(\Omega).$$

It is clear that compatible initial data for (3) leaves in K , so that the limit of the solution of (2), when $g \notin K$, is singular: letting $p \rightarrow \infty$, turns out to grow up a boundary layer connecting g to the limit. In [6] (see also [3]), it is proved that the limiting function is $v(1)$ (independent of t), where v is the unique solution of

$$(4) \quad \begin{cases} v(t)/t - v_t(t) \in \partial \mathbb{I}_{\infty}(v(t)) & \text{a.e. } t \in (\delta, 1] \\ v(\delta) = \delta g \end{cases}$$

and $\delta = 1/\|\nabla g\|_{\infty}$, in the sense that $v \in W^{1,2}(\delta, 1; L^2(\Omega))$, $v(\delta) = \delta g$ and, for any $t \in (\delta, 1]$, $v(t)/t - v_t(t) \in \partial \mathbb{I}_{\infty}(v(t))$.

In terms of Monge Kantorovich mass transfer theory the equation (4) means that v is a potential corresponding to optimal moving the mass $\mu^+ = v(\cdot, t)/t dx$ to $\mu^- = v_t(\cdot, t) dx$.

As a consequence of [6] (see also [3]), we have the following characterization of mapping \mathbb{Q} in terms of evolution equation (4):

Theorem 1 ([6] and [3]) *For any $g \in L^2(\Omega)$, $\mathbb{Q}(g) = v(1)$, where v is the unique solution of (4).*

In [6], it is also proved that operator \mathbb{Q} is not the projection onto K , the set of stable sandpiles. In order to give the numerical analysis and simulation of the collapsing of a sandpile, we give, in this paper, a more precise description of \mathbb{Q} , in terms of a composition of projections onto interlocked convex sets of $L^2(\Omega)$, around convex K .

To set our main results, let us give some notations. For a given convex $C \subseteq L^2(\Omega)$, we denote by \mathbb{P}_C , the projection with respect to the L^2 norm on C , defined by:

$$z = \mathbb{P}_C(u) \Leftrightarrow z \in C, \int_{\Omega} (u - z)(v - z) \leq 0 \quad \text{for any } v \in C.$$

For a given $[a, b]$ compact interval of \mathbb{R} , we say that $(d_i)_{i=0}^n$ is an ε -discretization of (a, b) , provided $\varepsilon > 0$, $d_0 = a < d_1 < d_2 < \dots < d_n = b$ and $d_i - d_{i-1} \leq \varepsilon$, for any $i = 1, \dots, n$. Notice that, letting $\varepsilon \rightarrow 0$ in an ε -discretization of a fixed interval (a, b) , is equivalent to let $n \rightarrow \infty$. For any $d > 0$, we denote by $K(d)$, the convex set given by

$$K(d) = \left\{ z \in W^{1,\infty}(\Omega) ; |\nabla z| \leq d \right\}.$$

Theorem 2 *Let $g \in W^{1,\infty}(\Omega)$, $a := \|\nabla g\|_{\infty}$ and $(d_i)_{i=0}^n$ an ε -discretization of $(1, a)$. Then*

$$(5) \quad \mathcal{Q}(g) = \lim_{n \rightarrow \infty} \mathbb{P}_{K(1)} \mathbb{P}_{K(d_1)} \dots \mathbb{P}_{K(d_{n-2})} \mathbb{P}_{K(d_{n-1})} g.$$

Proof : For $i = 1, \dots, n$, let us denote by

$$u_i = \mathbb{P}_{K(d_{n-i})} u_{i-1} \quad \text{and } u_0 = g,$$

i.e.

$$u_i + \partial \mathbb{I}_{K(d_{n-i})}(u_i) \ni u_{i-1} \quad \text{for } i = 1, \dots, n,$$

and

$$\mathbb{P}_{K(1)} \mathbb{P}_{K(d_1)} \dots \mathbb{P}_{K(d_{n-2})} \mathbb{P}_{K(d_{n-1})} g = u_n.$$

Setting, for $i = 1, \dots, n$,

$$z_i = u_i / d_{n-i},$$

it is not difficult to see that

$$(6) \quad z_i + \partial \mathbb{I}_{K(1)}(z_i) \ni \frac{d_{n-i+1}}{d_{n-i}} z_{i-1}.$$

Now, setting

$$t_i = 1/d_{n-i} \quad \text{for } i = 0, \dots, n,$$

it is clear that $(t_i)_{i=0}^n$ is an ε -discretization of $(\delta, 1)$. So that, the ε -approximate solution of

$$\begin{cases} v_i(t) + \partial \mathbb{I}_{\infty}(v(t)) \ni f(t) & \text{a.e. } t \in (\delta, 1] \\ v(\delta) = \delta g, \end{cases}$$

with $f(t) = v(t)/t$, associated with $(t_i)_{i=0}^n$ converges to v in $\mathcal{C}([\delta, 1]; L^2(\Omega))$. More precisely, taking the Euler implicit discretization in time

$$(7) \quad v_i + \partial \mathbb{I}_{K(1)}(v_i) \ni v_{i-1} + \frac{t_i - t_{i-1}}{t_{i-1}} v(t_{i-1}), \quad i = 1, 2, \dots, n,$$

where, we used the discretization of f given by $f_i = \frac{v(t_{i-1})}{t_{i-1}}$, for $i = 1, \dots, n$, and defining ε -approximate solution v_ε by $v_\varepsilon(t) = v_i$ for $t \in [t_i, t_{i+1}]$ for $i = 0, 1, \dots, n-1$, we have

$$(8) \quad v_\varepsilon \rightarrow v \quad \text{in} \quad \mathcal{C}([\delta, 1]; L^2(\Omega)), \text{ as } \varepsilon \rightarrow 0,$$

and

$$(9) \quad v_n \rightarrow v(1) \quad \text{in} \quad L^2(\Omega), \text{ as } n \rightarrow \infty.$$

Moreover, it is not difficult to see that (7) is equivalent to

$$v_i + \partial \mathbb{I}_{K(1)}(v_i) \ni \frac{d_{n-i+1}}{d_{n-i}} v_{i-1} + \frac{t_i - t_{i-1}}{t_{i-1}} (v(t_{i-1}) - v_{i-1}),$$

so that, by using (6) and the L^2 -contraction property of $(I + \partial \mathbb{I}_{K(1)})^{-1}$, for $i = 1, \dots, n$, we get

$$(10) \quad \begin{aligned} \|v_i - z_i\|_2 &\leq \frac{d_{n-i+1}}{d_{n-i}} \|v_{i-1} - z_{i-1}\|_2 + \frac{t_i - t_{i-1}}{t_{i-1}} \|v(t_{i-1}) - v_{i-1}\|_2 \\ &\leq \frac{t_i}{t_{i-1}} \|v_{i-1} - z_{i-1}\|_2 + \frac{t_i - t_{i-1}}{t_{i-1}} \|v(t_{i-1}) - v_{i-1}\|_2. \end{aligned}$$

Since, $v_0 = z_0 = g$, then iterating (10) for $i = n, \dots, 1$, we obtain

$$\begin{aligned} \|v_n - z_n\|_2 &\leq \sum_{i=2}^n \frac{t_n}{t_{n-i+1}} \frac{t_{n-i+1} - t_{n-i}}{t_{n-i}} \|v(t_{n-i}) - v_{n-i}\|_2 + \frac{t_n - t_{n-1}}{t_{n-1}} \|v(t_{n-1}) - v_{n-1}\|_2 \\ &\leq \frac{1}{\delta^2} \sum_{i=2}^{n-1} (t_{n-i+1} - t_{n-i}) \|v(t_{n-i}) - v_{n-i}\|_2 + \frac{1}{\delta} (t_n - t_{n-1}) \|v(t_{n-1}) - v_{n-1}\|_2 \\ &\leq \frac{1}{\delta^2} \sum_{i=0}^{n-1} (t_{n-i+1} - t_{n-i}) \|v(t_{n-i}) - v_{n-i}\|_2 \\ &\leq \frac{1}{\delta^2} \sum_{i=1}^{n-1} (t_{i+1} - t_i) \|v(t_i) - v_i\|_2, \end{aligned}$$

where we used the fact that, for any $k = 0, \dots, n$, $\delta \leq t_k \leq 1$ and $1/t_k \leq 1/\delta \leq 1/\delta^2$. Considering \bar{v}_ε given by $\bar{v}_\varepsilon(t) = v(t_i)$ for $t \in [t_i, t_{i+1}[$ and $i = 0, 2, \dots, n-1$, we obtain

$$\begin{aligned} \|v_n - z_n\|_2 &\leq \frac{1}{\delta^2} \sum_{i=0}^{n-1} \int_{t_i}^{t_{i+1}} \|\bar{v}_\varepsilon(t) - v_\varepsilon(t)\|_2 dt \\ &\leq \frac{1}{\delta^2} \int_\delta^1 \|\bar{v}_\varepsilon(t) - v_\varepsilon(t)\|_2 dt \end{aligned}$$

Since, as $\varepsilon \rightarrow 0$, $\bar{v}_\varepsilon \rightarrow v$ and $v_\varepsilon \rightarrow v$ in $\mathcal{C}([\delta, 1]; L^2(\Omega))$, then

$$\lim_{n \rightarrow \infty} \|v_n - z_n\|_2 = 0.$$

At last, since $z_n = u_n/d_0 = u_n$, then by using (9), we deduce that, as $n \rightarrow \infty$,

$$u_n \rightarrow v(1) \quad \text{in} \quad L^2(\Omega),$$

and (5) follows. ■

2. Numerical approximations

2.1 The numerical problem

Let $g \in W^{1,\infty}(\Omega)$ be given. Our aim in this section is to give a numerical approximation of $\mathbb{Q}(g)$. By using Theorem 2, it is clear that it is enough to find an numerical method to compute the projection of a given function, that we call g again, on a convex $K_{(d)}$ with arbitrary $d \geq 1$.

In [5], we gave a numerical method based on duality arguments for numerical approximation of the projection on the convex $K_{(1)}$. Even if the context here is different, we are going to use the same method for our situation. Remember that

$$(11) \quad u = \mathbb{P}_{K_{(d)}}(g)$$

is equivalent to

$$J(u) = \inf\{J(v), v \in W^{1,\infty}(\Omega)\}$$

where $J(v) = \frac{1}{2}\|v - g\|_{L^2}^2 + \mathbb{I}_{K_{(d)}}(v)$. In, [5], we have proved that:

$$(12) \quad \min_{v \in W^{1,\infty}(\Omega)} J(v) = \sup_{q \in H_{div}(\Omega)} -G(q)$$

where

$$G(q) = \frac{1}{2} \int_{\Omega} |div q|^2 + \int_{\Omega} g \, div q + \int_{\Omega} |q|$$

and

$$H_{div}(\Omega) = \{q \in (L^2(\Omega))^2, div(q) \in L^2(\Omega)\}.$$

Remember also, that in general $\sup_{q \in H_{div}(\Omega)} -G(q)$ is not reached in $H_{div}(\Omega)$. Indeed,

there exists σ a \mathbb{R}^N -vector valued Radon measure such that $div(\sigma) \in L^2(\Omega)$, $u = \mathbb{P}_{K_{(d)}}g = g - div\sigma$ in $\mathcal{D}'(\Omega)$ and σ is related to the tangential derivative of u with respect to $|\sigma|$, the total variation measure associated to σ (cf. [4]). For the exact description of σ one can see the paper [11] for equivalent formulations in divergence form of equation $v \in \partial \mathbb{I}_{K_{(d)}}f$.

So, an numerical approximation of $\mathbb{P}_{K_{(d)}}g$ will follow by approximating $\sup_{q \in H_{div}(\Omega)} -G(q)$ and computing $g - div(q)$. Coming back to the numerical approxi-

mation of $\mathbb{Q}(g)$, we take $(d_i)_{i=0}^n$ an ε -discretization of interval $(1, \|g\|_{\infty})$, with a given small $\varepsilon > 0$; i.e. a large n , and we use the algorithm of approximation of $\mathbb{P}_{K_{(d)}}g$, to approximate composition

$$\mathbb{P}_{K_{(1)}}\mathbb{P}_{K_{(d_1)}}\dots\mathbb{P}_{K_{(d_{n-2})}}\mathbb{P}_{K_{(d_{n-1})}}g.$$

2.2 Space discretization

The solution of dual problem (12) is computed using Raviart Thomas finite element of the lowest order [12]. Denoting by h the average length of the elements, V_h the space of finite elements and σ_h the solution of problem

$$(13) \quad G(\sigma_h) = \inf_{q_h \in V_h} G(q_h),$$

the convergence of σ_h to σ is guaranteed remarking that we have

$$\|\sigma_h - \sigma\|_{L^2} \leq \|r_h(\sigma_p) - \sigma\|_{L^2}$$

where r_h is the projection onto V_h .

Finally, the minimization of G on V_h is implemented using a relaxation procedure.

3. Numerical results

In this section we present some numerical results on collapsing sandpiles.

3.1 The one dimensional case

First, we study example given in [6], where the stable sandpile is not the projection of the initial data. More precisely, the unstable initial data is composed in the following manner: two sandpiles with sides of slope equal to 2, with a width equal to 0.2, and centered around $x_0 = \pm 0.22$; and one sandpile with sides of slope equal to 250, with a width equal to 0.008 and centered around $x = 0$. The spacial discretization of the problem is carried out using $N = 2500$ points.

The maximal slope of this sandpile is $|\nabla g|_\infty = \bar{\theta} = 250$.

Figure 1 presents solutions obtained using different uniform discretizations of interval $[1, \bar{\theta}]$. In others words, decreasing maximal slope θ_i for sequence of projections is chosen such that $\theta_i = 1 + i \frac{\bar{\theta}-1}{M}$ for $i = 1, \dots, M$. In the numerical experiments, the number M of projections is ranging from 1 to 5000.

One can observe that if we do a direct projection on $K(1)$ ($M = 1$), then the numerical final stable sandpile is composed of three adjacent sandpiles. When number M of subdivisions increases, the central small triangle disappears.

These numerical results corroborate the theoretical results given in [6], where it is shown that in this case, the stable sandpile consists of two adjacent triangles.

3.2 The two dimensional case

This paragraph is devoted to the two dimensional computations.

First, figure 3 shows the convergence rate of the approximation of one projection, when the average step of discretization tends to zero. In this computation, domain Ω is unit square $(-1, 1)^2$, discretized with squares $[-1 + ih, -1(i + 1)h] \times [-1 + jh, -1 + (j + 1)h]$, with $h = \frac{2}{N}$ and $0 \leq i, j \leq N$ for a given integer N .

Initial data g is a cone centered on the origin with radius of the basis equal to $R = \frac{1}{4}$, height $H = 1$ (see figure 2, up), and exact solution u is a cone centered on the

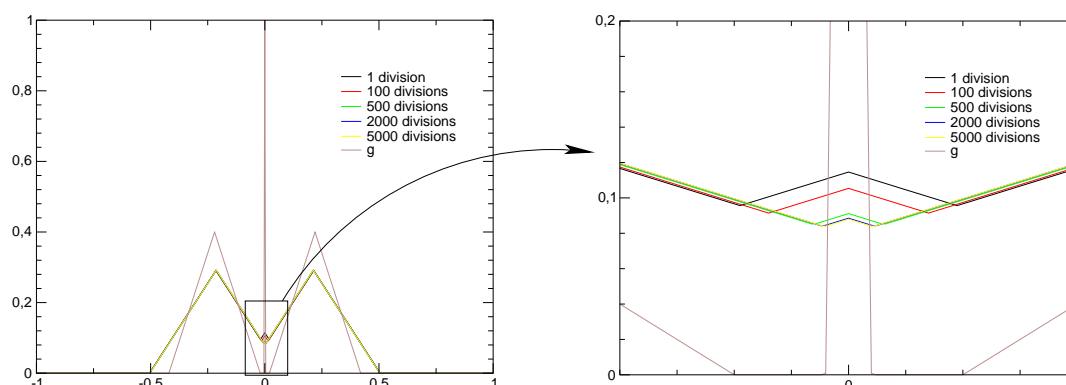


Figure 1: The counterexample where the final stable sandpile is not the direct projection of the initial unstable sandpile (details on the right)

origin with radius of the basis \tilde{R} and height \tilde{H} equal to $\tilde{R} = \tilde{H} = 2^{-\frac{4}{3}} \simeq 0.397$ (see figure 2, down).

Results plotted in figure 3 shows the L^2 -norm of the error $\|u_N - u\|_{L^2(\Omega)}$ where u_N is the computed solution, versus number $N = \frac{2}{h}$ of squares used for the discretization in each direction. This figure shows that the convergence rate of the error verifies $\|u_N - u\|_{L^2(\Omega)} = O(N^{-\alpha})$ with $\alpha \simeq 1.92$, when N is ranging from 50 to 150.

We present here a result with a more complex initial unstable sandpile, plotted in figure 4. The maximal slope of this sandpile is equal to $|\nabla g|_\infty = 4.1$, and the maximal slope of the final stable sandpile is equal to $|\nabla u|_\infty = 0.4$.

Remarks *In the theoretical part of this article, for seek of simplicity, angle α of the maximal slope of stability has been taken equal to $\alpha = \frac{\pi}{4}$ (see formula (1) for example), but the results presented here are true with any angle $\alpha \in (0, \frac{\pi}{2})$. Here, we have chosen $\alpha \simeq \frac{\pi}{8}$.*

Two different boundary conditions are considered to compute the projection:

- First, we take the Dirichlet boundary condition: $u(x) = 0$ on $\partial\Omega$. This simulates the experiment where the sandpile collapses on a table. The result is plotted in figure 5.
- Then, we consider the Neumann boundary condition: $m\partial_n u = 0$ on $\partial\Omega$. This simulates the case where domain Ω is the bottom of a box. Here, the mass has to be conserved. The final stable sandpile is plotted in figure 6. The initial and the final sandpile has a volume equal to 0.62178, which shows that the volume is numerically conserved.

These results are obtained using a spacial discretization with $N = 100$ and a number of emboities projections equal to $M = 40$. In this case, the result does not depend on M .

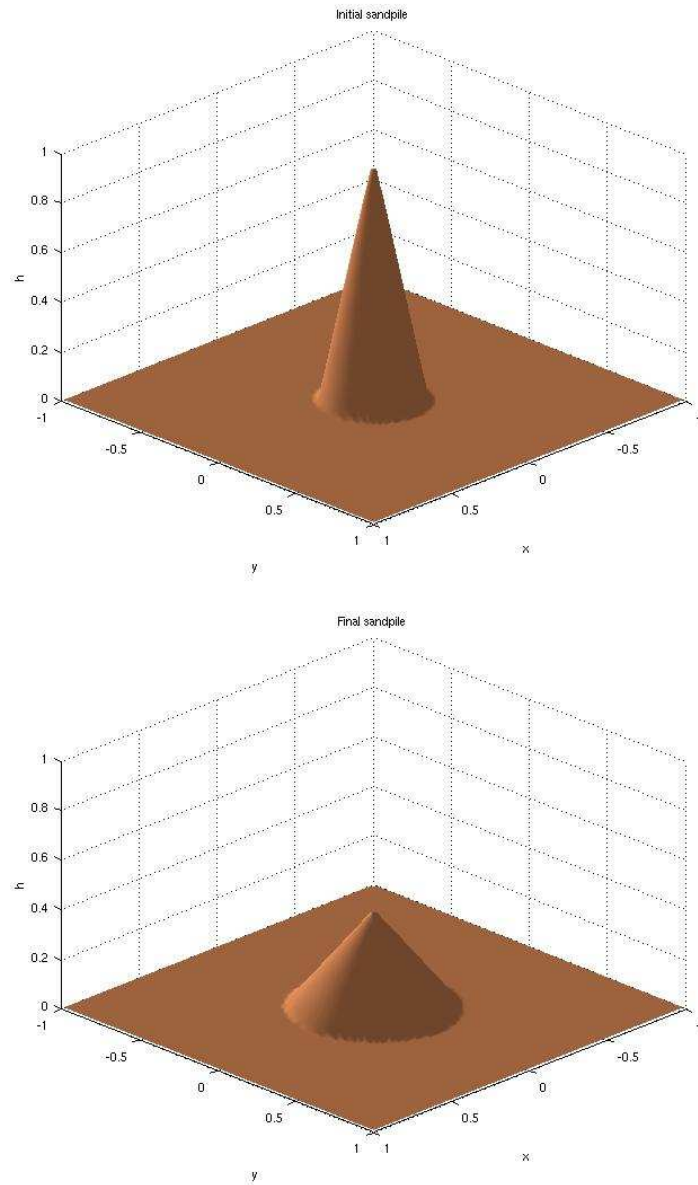


Figure 2: Initial unstable (up) and final stable (down) sandpile

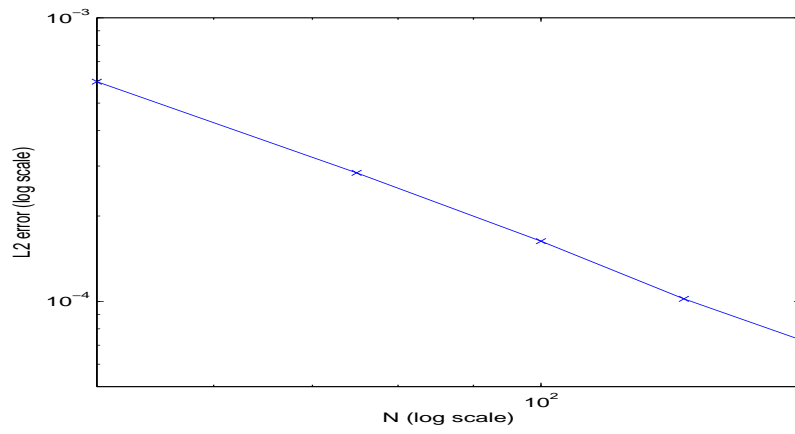


Figure 3: Accuracy of the method (L^2 -norm of the difference between the exact and the computed solution)

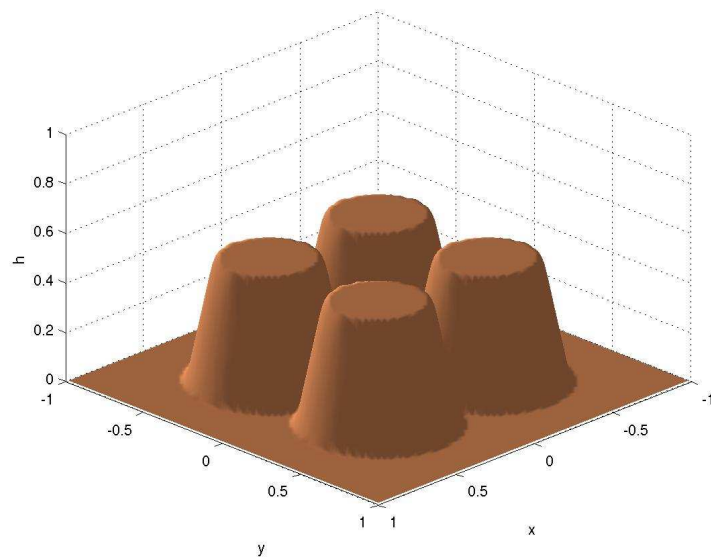


Figure 4: Initial unstable sandpile

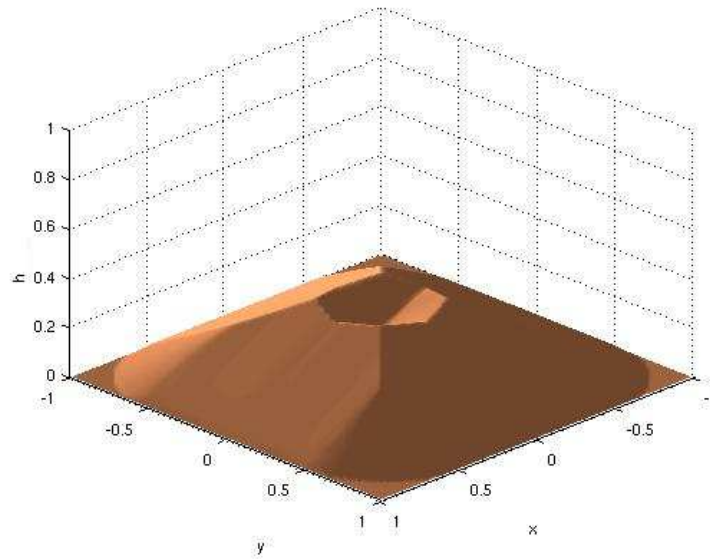


Figure 5: Collapsing sandpile with Dirichlet boundary condition

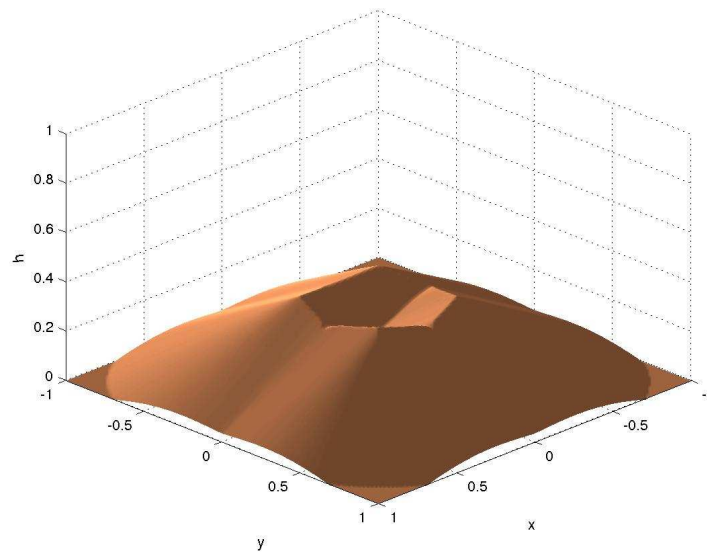


Figure 6: Collapsing sandpile with Neumann boundary condition

References

- [1] L. De Pascale, L. C. Evans and A. Pratelli, Integral estimates for transport densities, *Bull. London Math. Soc.*, **36**, 3, 383-395, 2004.
- [2] J. W. Barrett and L. Prigozhin, Dual formulation in Critical State Problems, *Interfaces and Free Boundaries*, **8**, 349-370, 2006.
- [3] Ph. Bénilan, L. C. Evans and R. F. Gariepy, On some singular limits of homogeneous semigroups, *J. Evol. Equ.*, **3** (2003), no. 2, 203–214.
- [4] G. Bouchitté, G. Buttazzo and P. Seppecher, Energies with respect to a Measure and Applications to Low Dimensional Structures, *Calc. Var. Partial Differential Equations* 5 (1997), 37-54.
- [5] S. Dumont and N. Igbida, Back on a Dual Formulation for the Growing Sandpile Problem, *Preprint*, 2007.
- [6] L. C. Evans, M. Feldman and R. F. Gariepy, Fast/Slow diffusion and collapsing sandpiles, *J. Differential Equations*, **137**:166–209, 1997.
- [7] L. C. Evans and W. Gangbo, Differential equations methods for the Monge-Kantorovich mass transfer problem, *Mem. Am. Math. Soc.*, **137**, no. 653, 1999.
- [8] I. Ekeland and R. Témam, Convex analysis and variational problems, *Classics in Applied Mathematics, Society for Industrial and Applied Mathematics (SIAM), Philadelphia, PA, 1999*.
- [9] L. C. Evans, J.-L. Lions et R. Trémollières, Partial differential equations and Monge-Kantorovich mass transfer, *Current Developments in Mathematics*, Int. Press, Boston, Ma, (1997) 65-126.
- [10] R. Glowinski, J.-L. Lions and R. Trémollières, Analyse numérique des inéquations variationnelles, *Méthodes Mathématiques de l'Informatique, Dunod, Paris, 1976*.
- [11] N. Igbida, On Monge-Kantorovich Equation, *Preprint*, 2008.
- [12] J.E. Roberts and J.-M. Thomas, Mixed and hybrid methods, P.G. Ciarlet, J.L. Lions (Eds.), *Handbook of Numerical Analysis*, vol. II, Finite Element Methods (Part 1), North-Holland, Amsterdam, 1991.